Polyaminoanthraquinone with Modulated Iminium Electron Delocalization for Efficient Electrochemical Ammonium Removal

Fei Yu[1,3], Tianjie Chen[1], Jinfeng Chen[2], Shuzhen Liang[3], Peng Liu[5], Jie Ma[2,3,4*]

[1] College of Oceanography and Ecological Science, Shanghai Ocean University, No 999, Huchenghuan Road, Shanghai, 201306, P. R. China.

[2] Research Center for Environmental Functional Materials, State Key Laboratory of Water Pollution Control and Green Resource Recycling, College of Environmental Science and Engineering, Tongji University, Shanghai, 200092, P. R. China.

[3] Water Resources and Water Environment Engineering Technology Center, Xinjiang Key Laboratory of Engineering Materials and Structural Safety, School of Civil Engineering, Kashi University, Kashi 844000, P. R. China.

[4] Shanghai Institute of Pollution Control and Ecological Security, Shanghai, 200092, P.R. China.

[5] Biolin (Shanghai) Trading Company Ltd, Rm 1205, Sandhill Plaza, Lane 2290 ZuChongzhi Road, Pudong New District, 201203 Shanghai China.

Corresponding author: Jie Ma, E-mail: jma@tongji.edu.cn, Tel: +86-021-65981

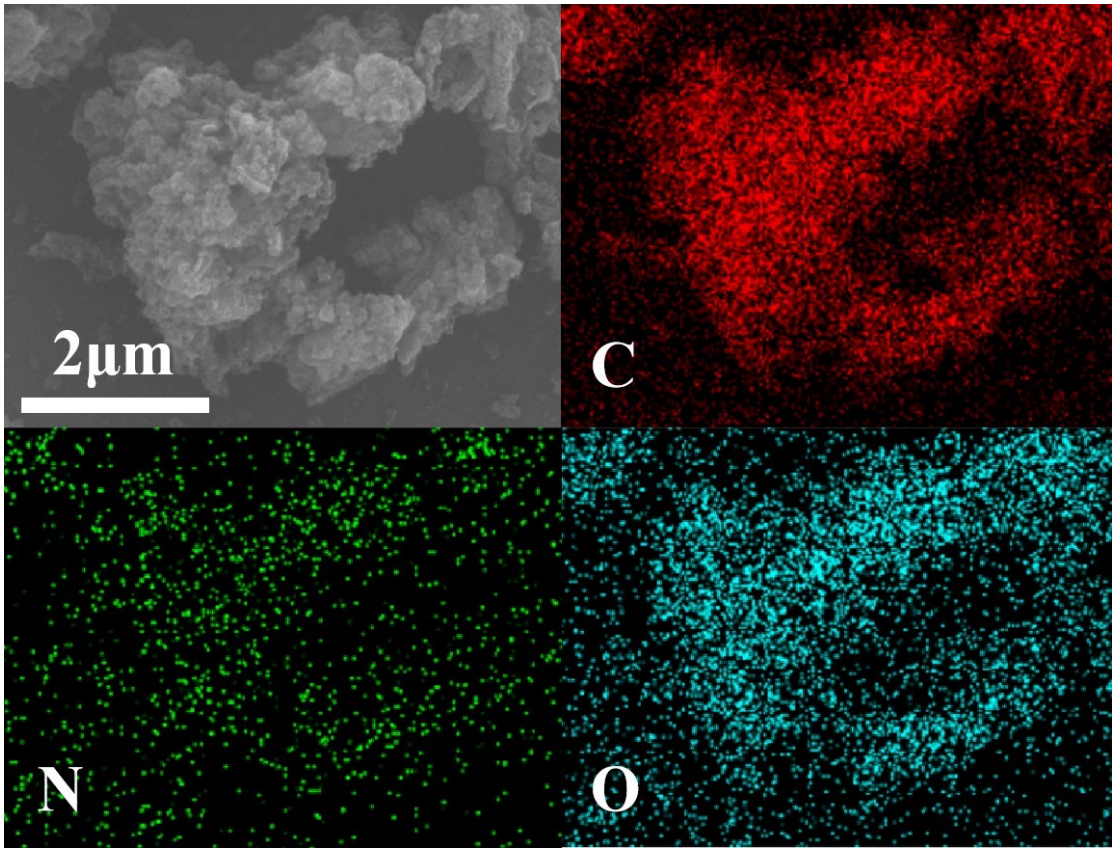

Fig. S1. SEM images of PAAQ and corresponding elemental mappings.

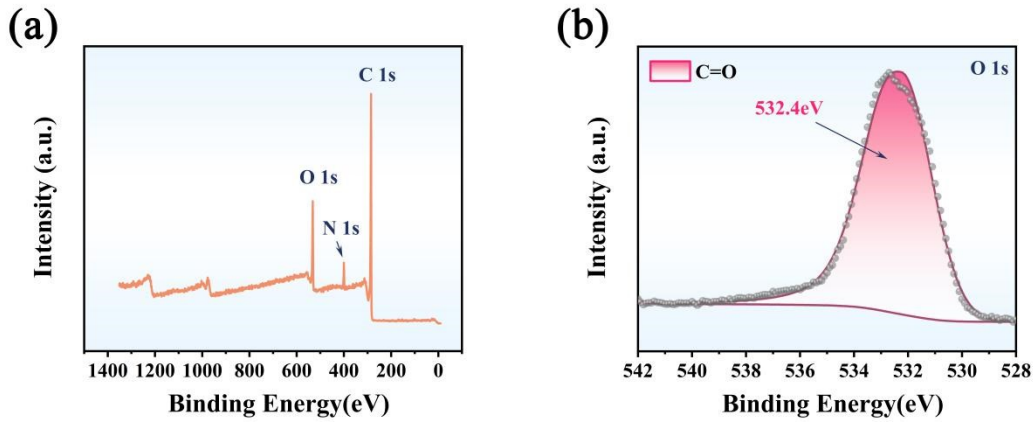

Fig. S2. (a) XPS survey spectra and (b) high-resolution XPS spectra of O 1s for the PAAQ.

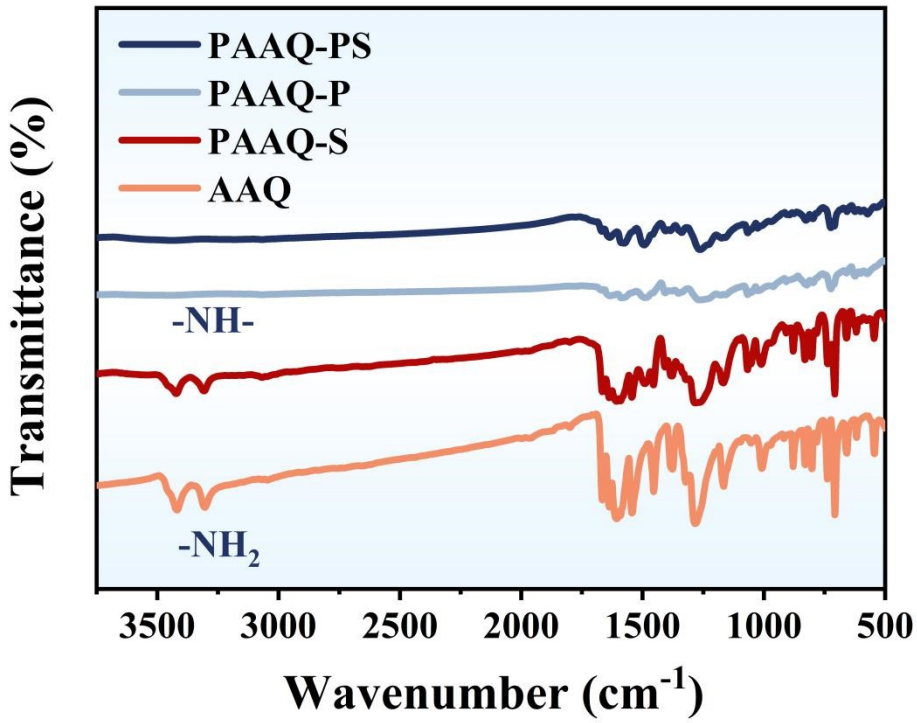

25

26 **Fig. S3.** FTIR spectroscopy of organic materials.

27

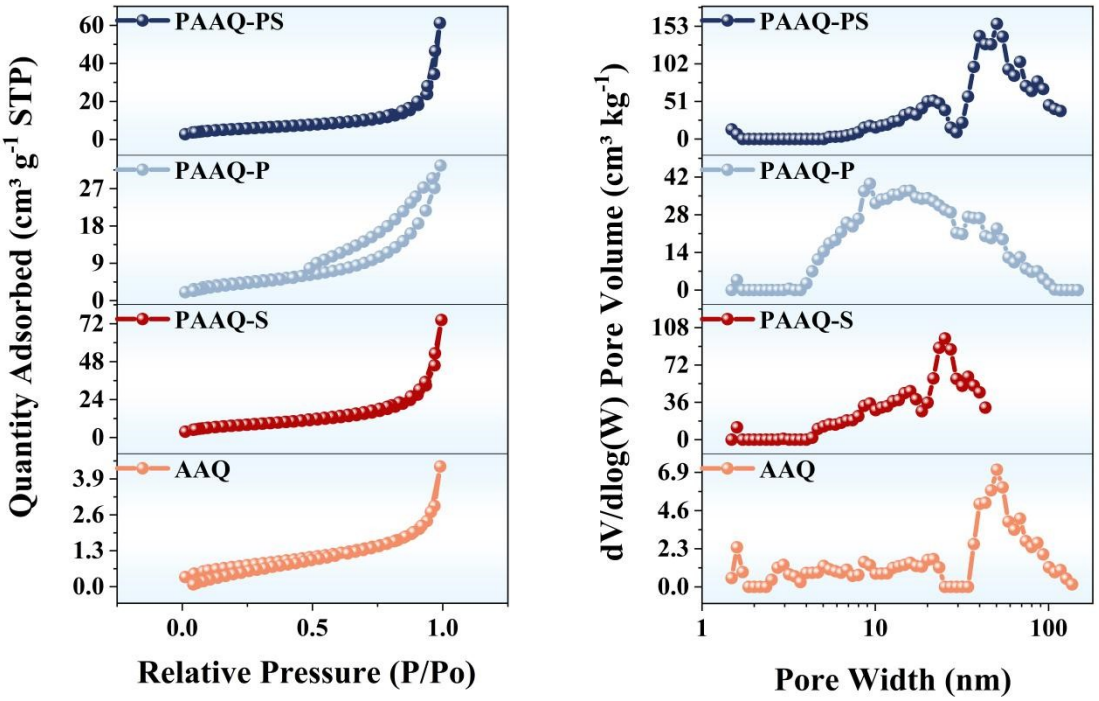

28

29 **Fig. S4.** (a) N_2 adsorption/desorption isotherms and (b) pore size distribution of organic materials.

30

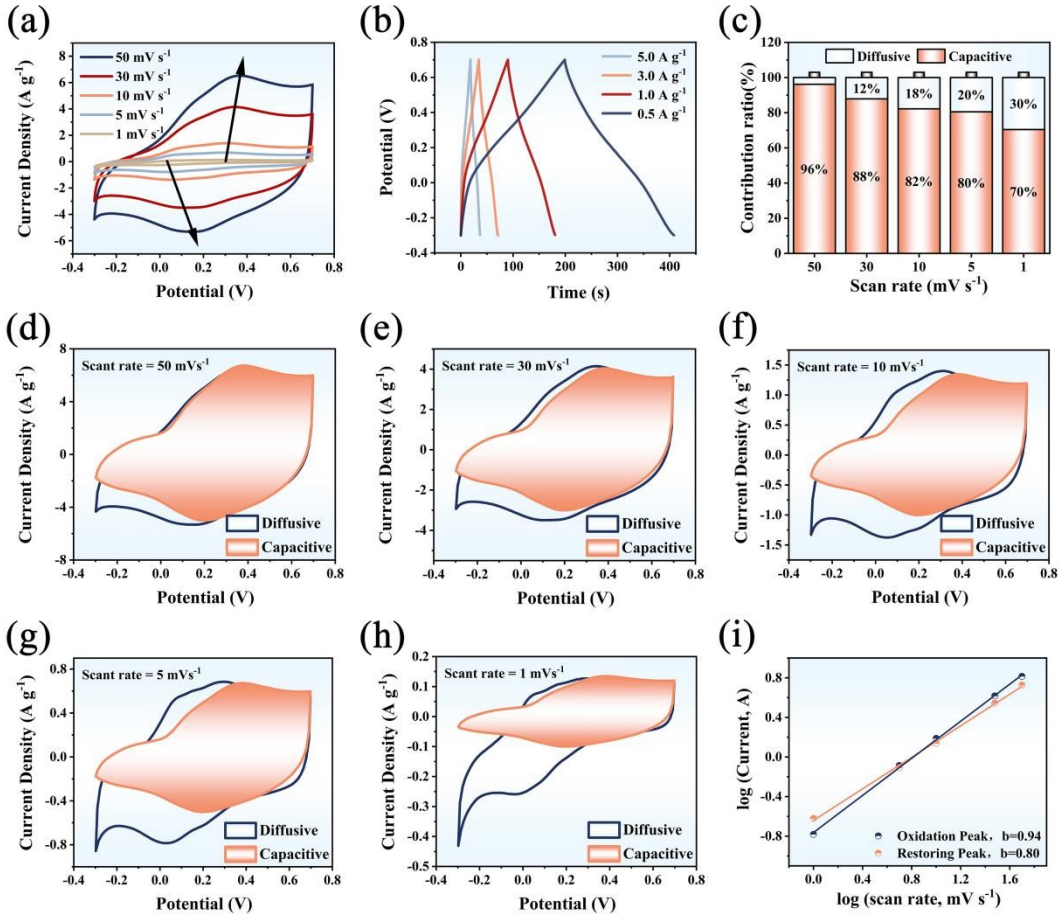

Fig. S5. (a) CV curves of PAAQ-PS in 1 M NH_4Cl solution under different scan rates. (b) GCD curves of PAAQ-PS at different specific currents. (c) Diffusion-limited and capacitive contributions to capacity of PAAQ-PS at different scan rates. (d-h) Capacitive contribution of PAAQ-PS at different scan rates. (i) Determination of b-values for various selected regions for PAAQ-PS.

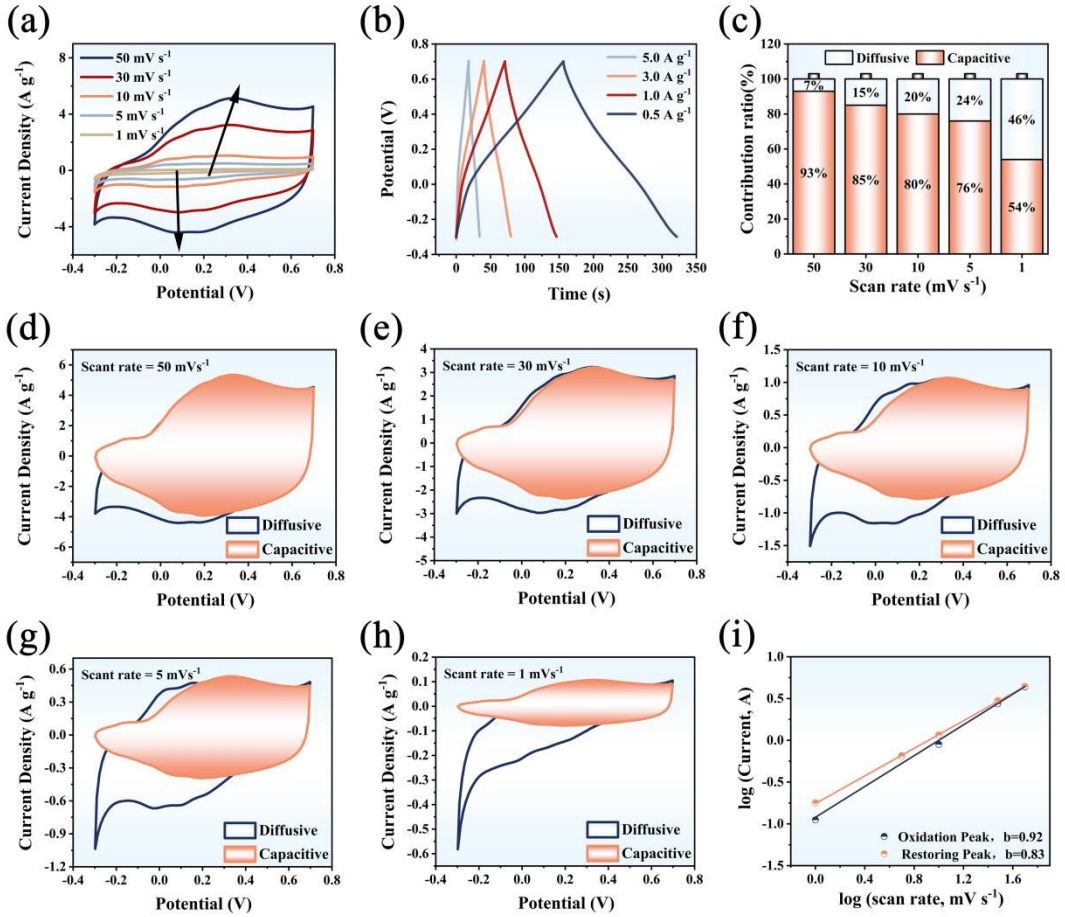

Fig. S6. (a) CV curves of PAAQ-P in 1 M NH_4Cl solution under different scan rates. (b) GCD curves of PAAQ-P at different specific currents. (c) Diffusion-limited and capacitive contributions to capacity of PAAQ-P at different scan rates. (d-h) Capacitive contribution of PAAQ-P at different scan rates. (i) Determination of b-values for various selected regions for PAAQ-P.

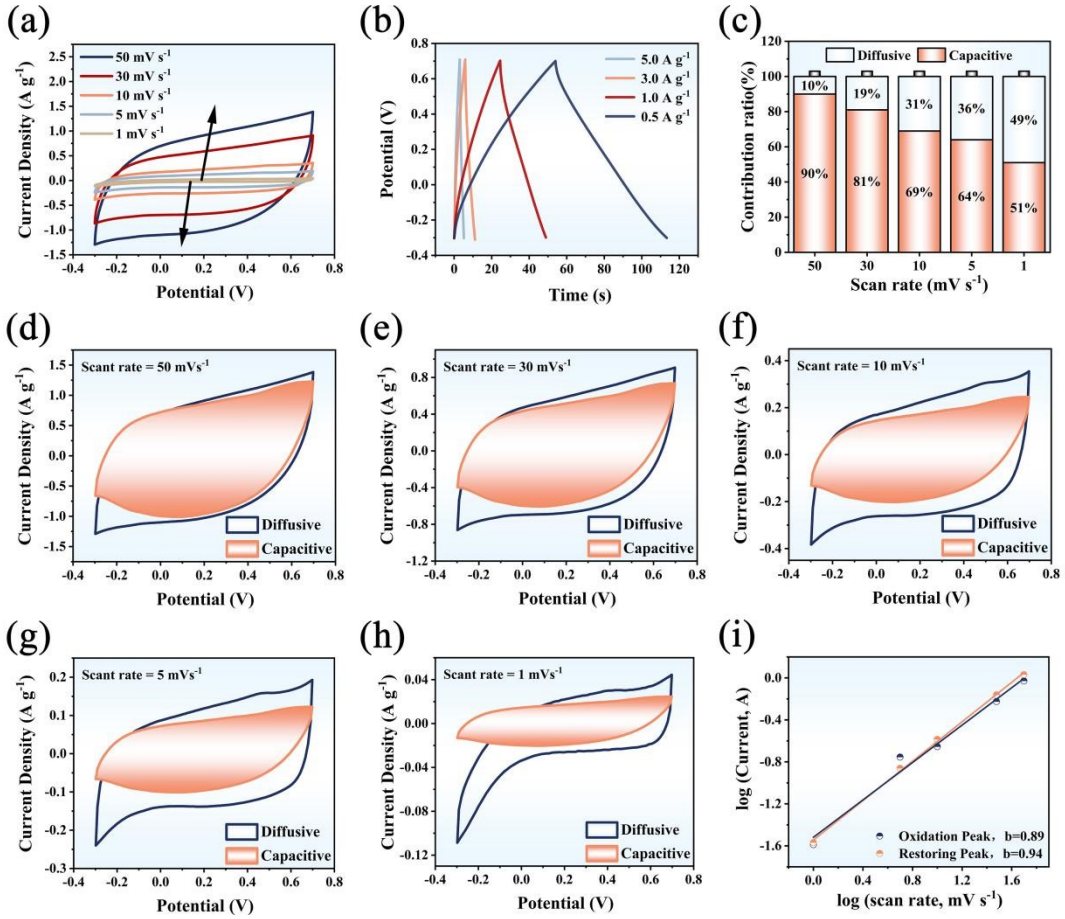

Fig. S7. (a) CV curves of PAAQ-S in 1 M NH_4Cl solution under different scan rates. (b) GCD curves of PAAQ-S at different specific currents. (c) Diffusion-limited and capacitive contributions to capacity of PAAQ-S at different scan rates. (d-h) Capacitive contribution of PAAQ-S at different scan rates. (i) Determination of b-values for various selected regions for PAAQ-S.

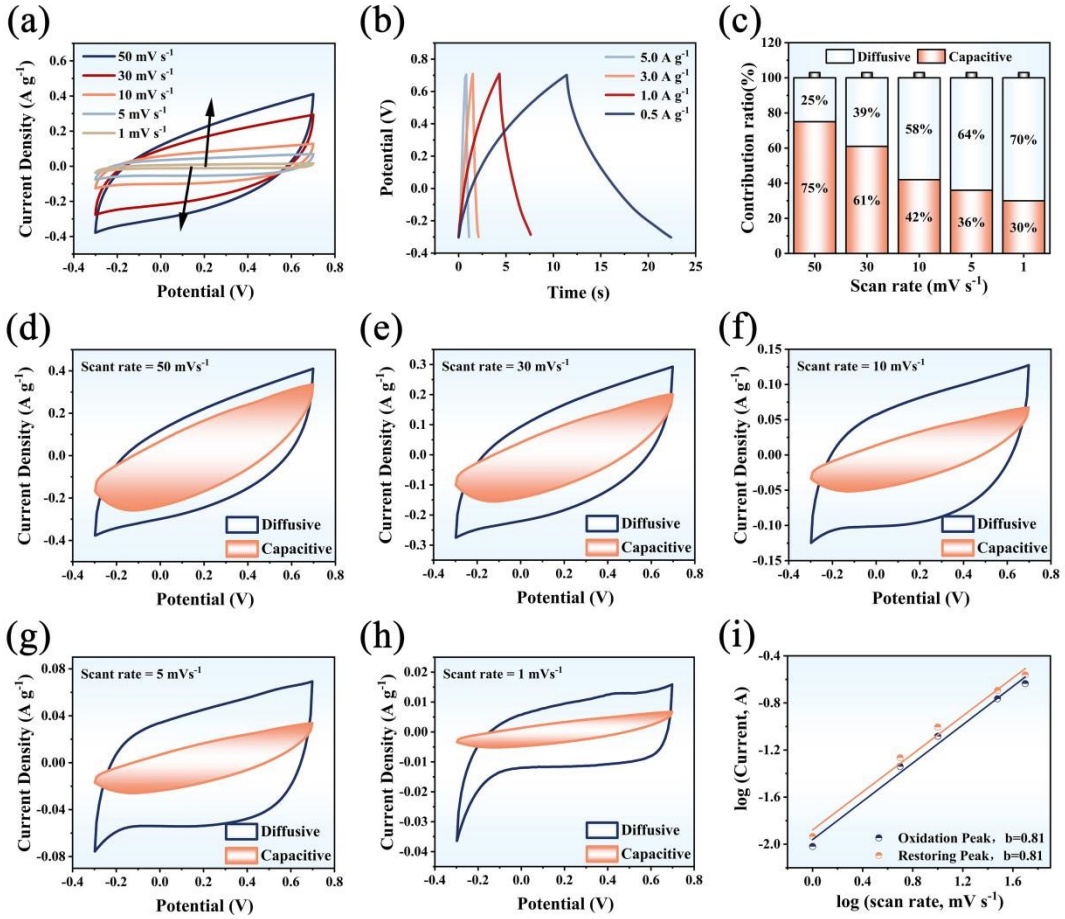

Fig. S8. (a) CV curves of AAQ in 1 M NH_4Cl solution under different scan rates. (b) GCD curves of AAQ at different specific currents. (c) Diffusion-limited and capacitive contributions to capacity of AAQ at different scan rates. (d-h) Capacitive contribution of AAQ at different scan rates. (i) Determination of b-values for various selected regions for AAQ.

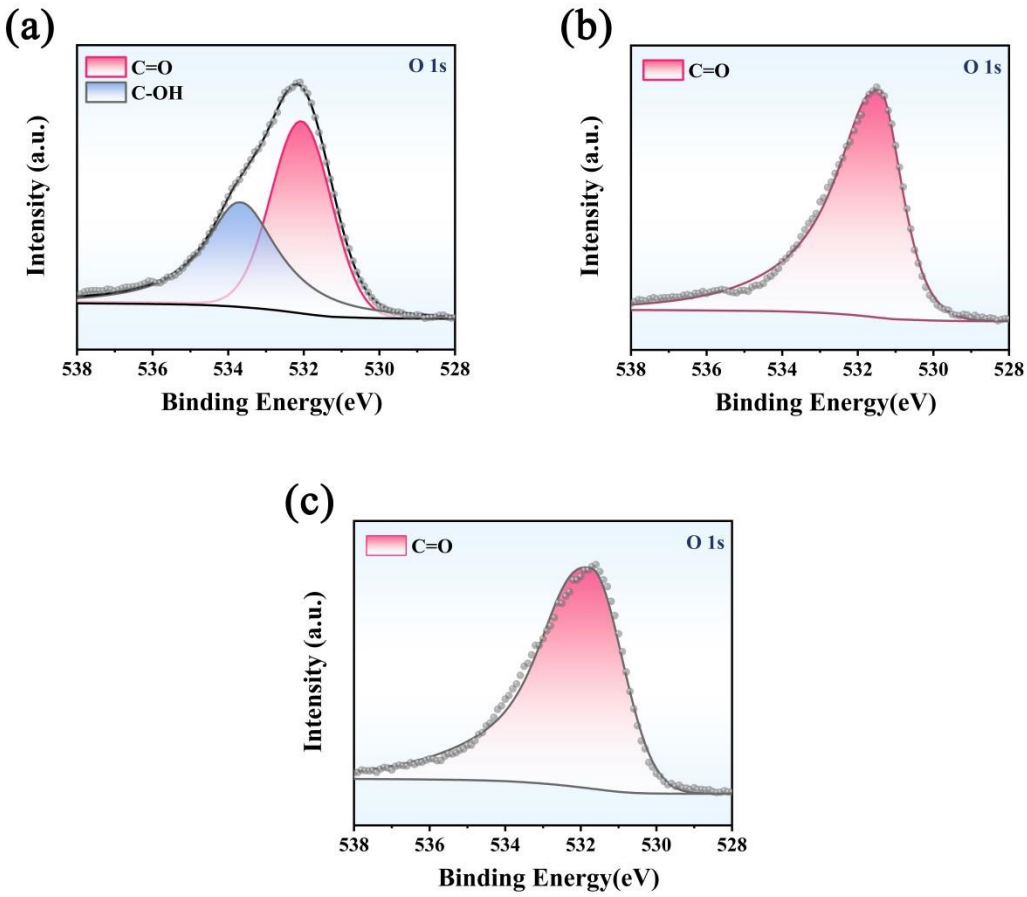

Fig. S9. High-resolution XPS spectra of O 1s for (a) PAAQ-P, (b) PAAQ-S and (c) AAQ after CDI.